IET Networks

Special Issue: Network Resource Optimisation with emphasis on Optical Networks

IET Journals
The Institution of Engineering and Technology

Analysing the optical network unit power consumption in the 10 GB-capable passive optical network systems

ISSN 2047-4954
Received on 23rd September 2015
Revised on 29th January 2016
Accepted on 20th February 2016
doi: 10.1049/iet-net.2015.0087
www.ietdl.org

Panagiotis Sarigiannidis[1] ✉, Malamati Louta[1], Georgios Papadimitriou[2], Michael Theologou[3]

[1]*Department of Informatics and Telecommunications Engineering, University of Western Macedonia, Kozani 50100, Greece*
[2]*Department of Informatics, Aristotle University, Thessaloniki 54124, Greece*
[3]*School of Electrical and Computer Engineering, National Technical University of Athens, Athens 15780, Greece*
✉ *E-mail: psarigiannidis@uowm.gr*

Abstract: The standardisation of the 10 GB-capable passive optical network (XG-PON) system is accompanied by a rigorous set of recommendations. Power reduction in XG-PONs is considered a quite important topic by the telecommunication standardisation sector (ITU-T), thus, with importance of energy saving, XG-PON recommendation describes power management processes in detail. The core power management process comprises distinct states representing the desired power management transitions, while two modes: namely, the doze and the cyclic sleep mode, are defined. This study provides an analytical model for power consumption computation of an optical network unit (ONU), assuming that the two modes are enabled in the ONU operation. The presented analytical findings are verified by conducting extensive simulation experiments. Concurrently, the average time spent on doze and cyclic sleep states is provided.

1 Introduction

Optical access networking technologies not only bear high rates of user bandwidth, but also look quite promising in the context of energy efficiency. Next-generation passive optical network (NG-PON), the most popular candidate of optical networking, has been considered as one of the most deliberate power consumer among all the access network technologies. Nevertheless, the proliferation of the NG-PON technologies involves a progressively increasing number of subscriber terminals, optical devices, and transceivers; thus, the related power consumption is expected to increase to a great extent [1].

Recently, the 10 GB-capable PON (XG-PON) was introduced as one of the most promising NG-PON systems. One of the most advanced features enhanced in the XG-PON system is the power saving support for efficient energy management. Specifically, low-power mode operation of network elements is enabled, switching specific network components of the access network to sleep mode so as to reduce energy consumption.

Considering the generic tree topology PON architecture, the optical line terminal (OLT), located at the central office, constitutes the tree 'root' providing access to the multiple optical network units (ONUs) via a point-to-multipoint optical fibre connection. Thus, a broadcast data delivery from the OLT to the ONUs is established, known as downstream direction, while data delivery from the ONUs to the OLT is referred to as upstream direction.

The XG-PON transmission convergence layer defines the specifications regarding power consumption. According to the ITU-T G.987.3 recommendations, two power saving modes are defined: the doze and the cyclic sleep modes [2, 3]. An ONU may experience three types of modes: namely, the normal (or awake) mode, in which the ONU is completely active, the doze mode, in which the ONU turns its transmitter off, and the cyclic sleep mode, during which the ONU deactivates both its transmitter and receiver.

Motivated by the power management framework, in this paper we endeavour to provide a rigorous analytical framework for computing the average ONU power consumption based on the telecommunication standardisation sector (ITU-T) recommendations. Even though the description of the ONU power management is comprehensive, to the best of our knowledge, a closed-form expression estimating the average power consumed by an ONU in an XG-PON system is not provided in related research literature. Accordingly, in this paper we aim to associate the power consumed by an ONU with the ONU traffic arrivals, mathematically modelling the power management state machine by using a discrete time Markov chain (DTMC). Beyond the average estimated power consumption of the ONU, we further estimate the average time spent in the doze mode and the cyclic sleep mode.

The remainder of this paper is organised as follows. Section 2 presents an overview of the related research literature. Section 3 describes the XG-PON power management process according to the ITU-T specifications. Section 4 elaborates on the proposed DTMC model along with the analytical framework. Section 5 validates the proposed model by means of extensive simulation experiments, considering several performance metrics. Finally, Section 6 concludes this paper and outlines our plans for future work.

2 Related work

Today, traditional energy resources such as hydrocarbon energy provide most of the energy demand, but this kind of energy is not renewable, and it is expected to be finally used up in the not-too-distant future. Moreover, the combustion of hydrocarbon materials releases large amounts of greenhouse gases, a major cause of global warming [4]. In [5], Zhang and Ansari discuss challenges and scheduling frameworks of the 10 Gbps Ethernet Passive Optical Network (EPON) (10G-EPON). Then, they focus on sleep-aware scheduling schemes for 10G-EPON systems. A power saving mechanism was proposed in [6]. The mechanism intends to apply a variable low-power period based on current traffic conditions. The performance of the proposed framework is assessed by simulation results. Adaptive link rate (ALR) control functions are discussed and proposed in [7]. The work is focused on 10G-EPON. ALR functions govern the downlink rate between the OLT and the ONUs based on the ongoing traffic density. Depending on the quantity of traffic, the line rate is switched to 1 or 10 Gbps. Simulation results validate the performance of the proposed functions. The trade-off between the energy savings and

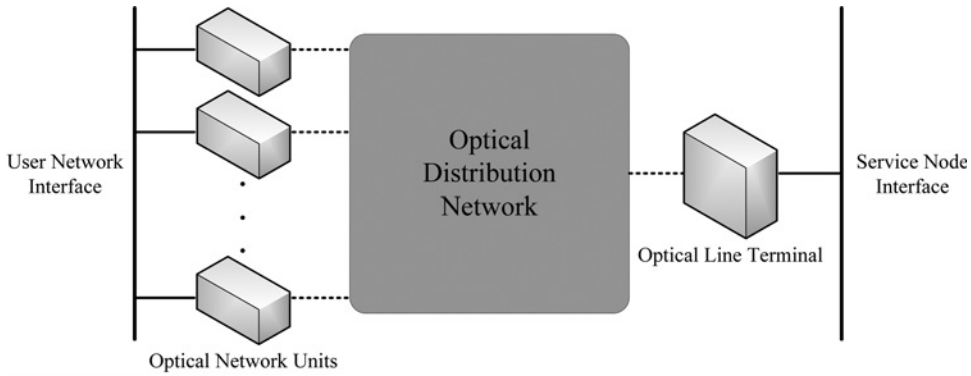

Fig. 1 *XG-PON network model*

the network performance is discussed in [8]. The slow transition of power from active mode to sleep mode, the recovery and the synchronisation overhead, and the additional packet delay when an optical unit is not switched properly are some of the key issues discussed in this paper. By judging the networks status, effort in [9] apply an energy-efficient scheme under multiple traffic scenarios. In [10], the energy reduction is investigated with respect to multicasting transmission. ONUs that are not included in the multicast group are switched to sleep mode. Simulation results indicate that the proposed scheme reduces the energy consumed subject to the ongoing broadcast transmission. The requirements of NG-PONs are raised in [11]. In addition, a generic power saving framework was introduced, based on the network units' dimensions that maintains the quality of service needs. Similarly, energy saving techniques are discussed in [12] assuming time division multiplexing (TDM) PONs. Various scenarios were considered where TDM traffic was utilised. According to the paper's findings, 50% energy saving are possible. In [13], a power saving algorithm based on the slow start scheme was proposed for EPON which adjusts the low-power period in accordance to the present traffic. Simulation results demonstrate the merits of the algorithm. Effort in [14] presented a downstream system model for EPONs which is able to calculate the expected mean packet delay. Then, identical transmission cycles are set in order to maximise the energy gains.

In [15], Bang *et al.* endeavour to determine the low-power period duration by defining a cost function. Assuming a Poisson process to model the inter-arrival procedure, the work studies the cyclic sleep mode impact on the network performance. Similar effort in [16] aim to determine the required ONU buffer size for effective implementation of the cyclic sleep mode. Their approach is based on an analytical model that realises the behaviour of an ONU being in cyclic sleep mode when upstream arrivals occur.

3 XG-PON power management

The ONU management and control interface (OMCI) constitutes the core signalling mechanism between the ONUs and the OLT. This mechanism is mainly governed by the OLT in order to manage the connected ONUs in the XG-PON system. The OLT is able to manage ONUs' connection and control the user network interface (UNI) via the OMCI. The UNI is the connection point between the ONU and the users that are attached to the ONU. The OLT uses OMCI to discover the ONUs' power management capabilities and to configure their power management attributes and modes [3]. Fig. 1 illustrates the generic XG-PON network model.

The XG-PON power management is structured in power state machines. The states are interconnected, forming two mutually exclusive subsets: the full power and the low-power subsets. The full power subset consists of two distinct management states: the *ActiveHeld* and the *ActiveFree* states. The *ActiveHeld* period incorporates awake mode with full power consumption. During the *ActiveFree* state, the ONU monitors the upstream traffic that arrives at the UNI and the downstream traffic that is collected by the service node interface (SNI) located at the OLT to be sent to the ONU in order to decide whether a low-power mode could be applied. The ONU in the *ActiveHeld* and the *ActiveFree* state consumes full power.

The low-power subset is realised by two low-power saving modes referred to as doze and cyclic sleep modes. During the cyclic sleep mode both transmitter and receiver are turned off, whereas in the doze mode the receiver remains turned on and the transmitter is turned off. Obviously, the ONU in doze mode is capable of receiving downstream traffic. The XG-PON power management defines two pairs of states for each low-power mode. In particular, the *DozeAware* and the *Listen* states constitute the doze mode, whereas the *SleepAware* and the *Asleep* states define the cyclic sleep mode. In essence, the *DozeAware* and *SleepAware* states are preparation states during which a decision is made on transiting or not to the *Listen* and the *Asleep* states by checking the upstream and both traffic streams, respectively. Even though the ONU maintains both transmitter and receiver turned on during the AwareStates, the power consumption is lightly reduced because the ONU partially operates.

On entering the *ActiveFree* state, the ONU begins to monitor the traffic that arrives. In case upstream traffic is sensed in the UNI, the ONU remains in full power mode; hence, the *ActiveHeld* follows the *ActiveFree* state. On the contrary, total absence of traffic during the *ActiveFree* period signals a potential cyclic sleep mode; thus, the ONU enters into the (initial) *SleepAware* state. If the absence of traffic continues during the initial *SleepAware* period, the ONU is set to cyclic sleep mode. Till the arrival of either upstream or downstream data streams, the ONU experiences an alternate sequence of *SleepAware* and *Asleep* states; during the *SleepAware* state, the ONU checks if there was any traffic during the previous *Asleep* state and itself for traffic presence. Any kind of traffic arrival leads the ONU to exit the cyclic sleep mode and return to the *ActiveHeld* state in awake mode. On the other hand, a doze mode is established in case the ONU experiences downstream, but no upstream traffic arrivals. In a similar manner to the cyclic sleep mode, an (initial) *DozeAware* state follows and an alternate sequence of *DozeAware* and *Listen* states is established, provided that no upstream traffic occurs. Again, the ONU enters into the *ActiveHeld* state on the reception of upstream traffic in the UNI. Fig. 2 illustrates the corresponding states of the power saving modes. At this point, it should be noted that there are two types of each Aware state; the initial Aware states decide on the sleep mode establishment based on the traffic sensed during the time period the corresponding Aware state lasts. Conversely to the Aware states during an ongoing low-power mode, i.e. those that follow a *Listen* or an *Asleep* state, wherein the continuation of the low-power mode in progress is based on the traffic sensed during the previous *Asleep* or *Listen* state plus the Aware state period itself. Thus, the *SleepAware* state is responsible for monitoring the downstream and upstream traffic during the last *Asleep* and the ongoing *SleepAware* state periods in order to decide on the cyclic sleep mode continuation, whereas the initial *SleepAware* state has to reach to a decision on the cyclic sleep

IET Netw., 2016, Vol. 5, Iss. 3, pp. 71–79

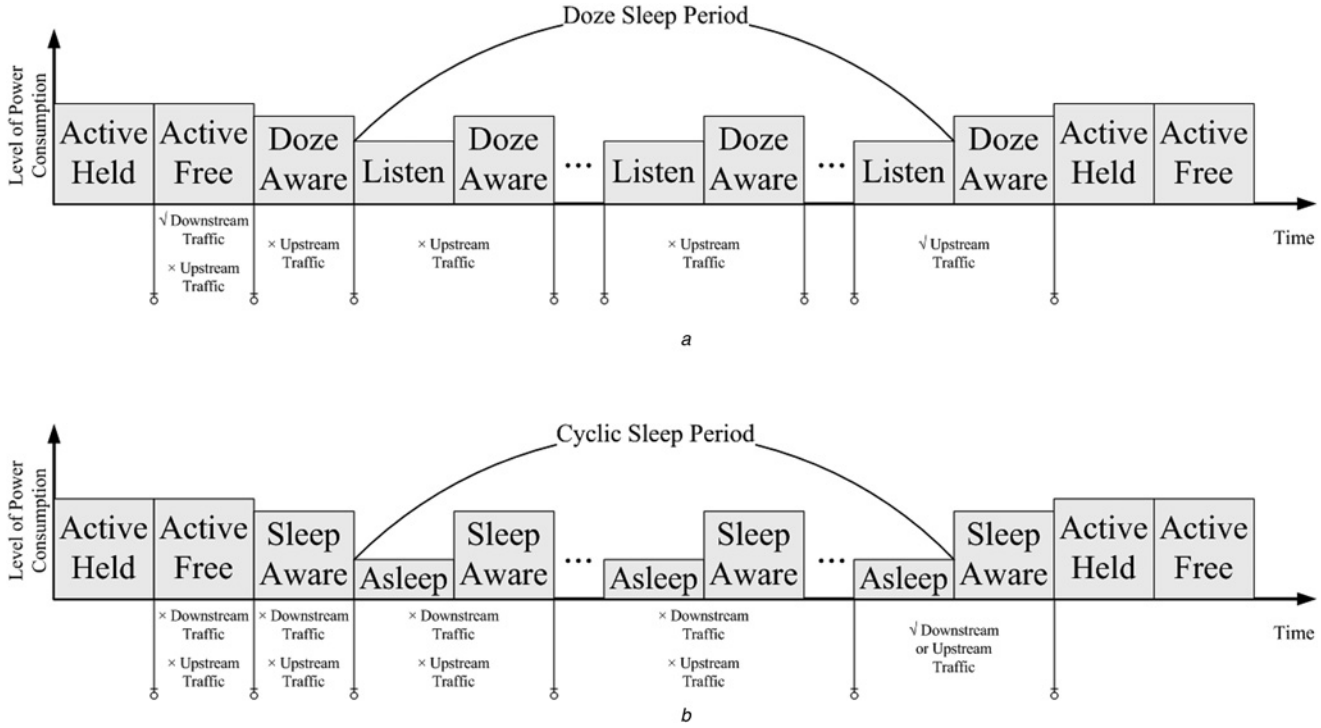

Fig. 2 *Power saving modes in XG-PON systems*

a Doze sleep period. The ONU enters a Listen period when there is absence of upstream traffic
b Cyclic sleep period. The ONU enters an asleep period when there is absence of both traffic streams

mode establishment based on the traffic monitored during its own time period. The same rationale stands for the *DozeAware* states.

The duration of each state is expressed as a multiplication of 125 μs periods of time (frames). The ONU maintains the ability to wake up on local stimuli stemming from physical layer operations, administration, or maintenance messages, also known as physical layer operations, administration and maintenance messages. On establishing a low-power mode, the doze or the cyclic sleep mode states are repeated until a local stimulus triggers the wake-up operation. Subsequently, the ONU enters the *ActiveHeld*.

4 XG-PON power management analysis

Let us consider an ONU connected to an XG-PON. The ONU is able to operate in all supported power management states, i.e. the *ActiveHeld*, the *ActiveFree*, the *DozeAware*, the *Listen*, the *SleepAware*, and the *Asleep* states. Let $\{\mathbf{PM}(t),\ t \in T\}$ denote the stochastic process reflecting the power management state of the ONU under consideration, where $T = \{0,\ 1,\ \ldots\}$. The state space of the stochastic process is discrete (the aforementioned six power management states are adopted in accordance with the ITU-T G.987.3 [2]). As already noted in the previous section, the initial *SleepAware*/initial *DozeAware* state is different from the *SleepAware*/*DozeAware* state that follow an *Asleep*/*Listen* state; thus, they should be distinguished in the stochastic process state definition. Hence, the state vector of the considered stochastic process is defined as follows: $\boldsymbol{S} = \{\boldsymbol{S}_1,\ \boldsymbol{S}_2,\ \boldsymbol{S}_3,\ \boldsymbol{S}_4,\ \boldsymbol{S}_5,\ \boldsymbol{S}_6,\ \boldsymbol{S}_7,\ \boldsymbol{S}_8\}$. This vector represents the ONU power management states as follows: *ActiveHeld* ($\boldsymbol{S}_1$), *ActiveFree* ($\boldsymbol{S}_2$), initial *DozeAware* ($\boldsymbol{S}_3$), *Listen* ($\boldsymbol{S}_4$), *DozeAware* ($\boldsymbol{S}_5$), initial *SleepAware* ($\boldsymbol{S}_6$), *Asleep* ($\boldsymbol{S}_7$), and *SleepAware* ($\boldsymbol{S}_8$).

To model the stochastic process $\mathbf{PM}(t)$ using a DTMC, the memoryless property should be ensured. More specifically, it should be ensured that there is no need to maintain knowledge concerning past transitions when the ONU makes transitions from one state to another. For example, the ONU should not maintain information concerning past transitions such as traffic arrivals. To this end, the following assumptions are adopted:

- Given that in XG-PON systems the downstream data delivery takes place in periodical downstream frames of 125 μs length, it is assumed that downstream traffic arrivals in SNI within a length of a downstream frame (125 μs) are fully accommodated in the following (downstream) frame. In other words, it is considered that buffers located in SNI at the OLT are emptied on the beginning of each following downstream frame. For example, the downstream frame has a fixed size of 135,432 bytes. In the context of this paper, we consider that this size is enough to cover all downstream traffic requests of all ONU within a downstream frame.
- Given that in XG-PON systems the upstream data delivery takes place in periodical upstream frames of 125 μs length, it is assumed that upstream arrivals in UNI within the length of an upstream frame (125 μs) are fully accommodated in the following (upstream) frame. Hence, ONU buffers in UNI are emptied in the beginning of each following upstream frame. Particularly, all upstream traffic requests are fulfilled within an upstream frame. For example, the upstream frame has a fixed size of 38,880 bytes. We consider that this capacity is enough to cover all upstream requests from all ONUs within an upstream frame.

Assuming the aforementioned remarks, the transition from state i to state j at time $t \in T$ (a) depends on the current state, i.e. state i and (b) is independent of time t. The ONU may experience any of the given power management states, i.e. enter any state at any time instance without any restriction. As a result, the stochastic process $\mathbf{PM}(t)$ constitutes a homogenous DTMC. Therefore, it holds $P\big(\mathbf{PM}(t+1) = j | \mathbf{PM}(t) = i\big),\ \ \forall t \in T$. Accordingly, the transition probability from state i to state j at time t is given as $p_{ij}(t) = P\big(\mathbf{PM}(t+1) = j | \mathbf{PM}(t) = i\big),\ \forall t \in T,\ \ i, j \in S$.
Considering DTMC properties, it follows that

$$\sum_{j=1}^{8} p_{ij} = 1,\ \forall\, i \in \boldsymbol{S} \tag{1}$$

$$0 \le p_{ij} \le 1,\ \forall (i, j) \in \boldsymbol{S} \times \boldsymbol{S} \tag{2}$$

The main notation of the DTMC model is summarised in Table 1.

Table 1 Model notation and parameters [2, 3]

Symbol	Description
$\mathbf{PM}(t)$	the stochastic process of the ONU power management
$T = \{0, 1, \ldots\}$	discrete time
$S = \{S_1, S_2, S_3, S_4, S_5, S_6, S_7, S_8\}$	state vector
p_{ij}	transition probability from state i to state j
u	stationary probabilities of the DTMC
Ξ	one-step transition matrix
λ_d	downstream arrival rate
λ_u	upstream arrival rate
P_{total}	total ONU power consumed in the XG-PON
M	number of ONUs in the network
P_c	average power consumption of the ONU
$P_{ah} = 4.69$ W	power consumed in the *ActiveHeld* state
$P_{af} = 4.69$ W	power consumed in the *ActiveFree* state
$P_{da} = 2.78$ W	power consumed in the *DozeAware* state
$P_{ls} = 1.7$ W	power consumed in the *Listen* state
$P_{sa} = 2.78$ W	power consumed in the *SleepAware* state
$P_{as} = 0.9$ W	power consumed in the *Asleep* state
$T_{ah} = 125$ μs	*ActiveHeld* state time period
$T_{af} = 125$ μs	*ActiveFree* state time period
$T_{da} = 125$ μs	*DozeAware* state time period
$T_{ls} = 125$ μs	*Listen* state time period
$T_{sa} = 125$ μs	*SleepAware* state time period
$T_{as} = 125$ μs	*Asleep* state time period

Fig. 3 depicts the state transition diagram of the proposed DTMC model. Initially, an ONU operates in *ActiveHeld* state. It remains in *ActiveHeld* state for a predefined time period equal to T_{ah} and then switches to *ActiveFree* state with probability $p_{12} = 1$. The ONU stays in *ActiveFree* state for T_{af} time. Thereafter, the ONU transits to one of three possible states as follows. First, it returns to the *ActiveHeld* state, if upstream traffic is monitored during T_{af} time with probability $p_{21} = A$. Second, a potential doze period is 'initiated' with the ONU entering the initial *DozeAware* state, in case downstream traffic is sensed in conjunction with the absence of upstream traffic. This probability is denoted by $p_{23} = B$. Third, the total absence of traffic received throughout T_{af} time leads to the initial *SleepAware* state with probability $p_{26} = 1 - A - B$. The possible transitions of the ONU being either in the initial *DozeAware* or in the initial *SleepAware* state are similar. In particular, $p_{34} = D$ stands for the probability of transiting from the initial *DozeAware* state to the *Listen* state in case no upstream traffic is monitored for the duration of the initial *DozeAware* state. Otherwise, i.e. in the case that upstream traffic is monitored, the ONU returns to the *ActiveHeld* state with probability $p_{31} = 1 - D$. Accordingly, the initial *SleepAware* state, with time period equal to T_{sa}, is connected to the *Asleep* state and to the *ActiveHeld* state with transition probabilities $p_{67} = C$ and $p_{61} = 1 - C$, in case no upstream and downstream traffic is observed or not, respectively. Finally, there is a circulation between both *DozeAware-Listen* and *SleepAware-Asleep* state pairs, where in the former case a doze mode is established and, thereafter, maintained as long as no upstream traffic appears, whereas in the latter case a cyclic sleep mode is initiated that persists up to the presence of either upstream or downstream traffic. To this end, $p_{54} = F$ and $p_{87} = E$ denote the probability of absence of upstream traffic and total traffic, respectively. The time period of the *Listen* and the *Asleep* states is denoted by T_{ls} and T_{as}, respectively. The transition matrix Ξ summarises the one-step transition probabilities

$$\Xi = \begin{bmatrix} 0 & 1 & 0 & 0 & 0 & 0 & 0 & 0 \\ A & 0 & B & 0 & 0 & 1-A-B & 0 & 0 \\ 1-D & 0 & 0 & D & 0 & 0 & 0 & 0 \\ 0 & 0 & 0 & 0 & 1 & 0 & 0 & 0 \\ 1-F & 0 & 0 & F & 0 & 0 & 0 & 0 \\ 1-C & 0 & 0 & 0 & 0 & 0 & C & 0 \\ 0 & 0 & 0 & 0 & 0 & 0 & 0 & 1 \\ 1-E & 0 & 0 & 0 & 0 & 0 & E & 0 \end{bmatrix}$$

The vector $\boldsymbol{u} = \{u_1, u_2, u_3, u_4, u_5, u_6, u_7, u_8\}$ is defined, representing the stationary probabilities of the DTMC. This vector

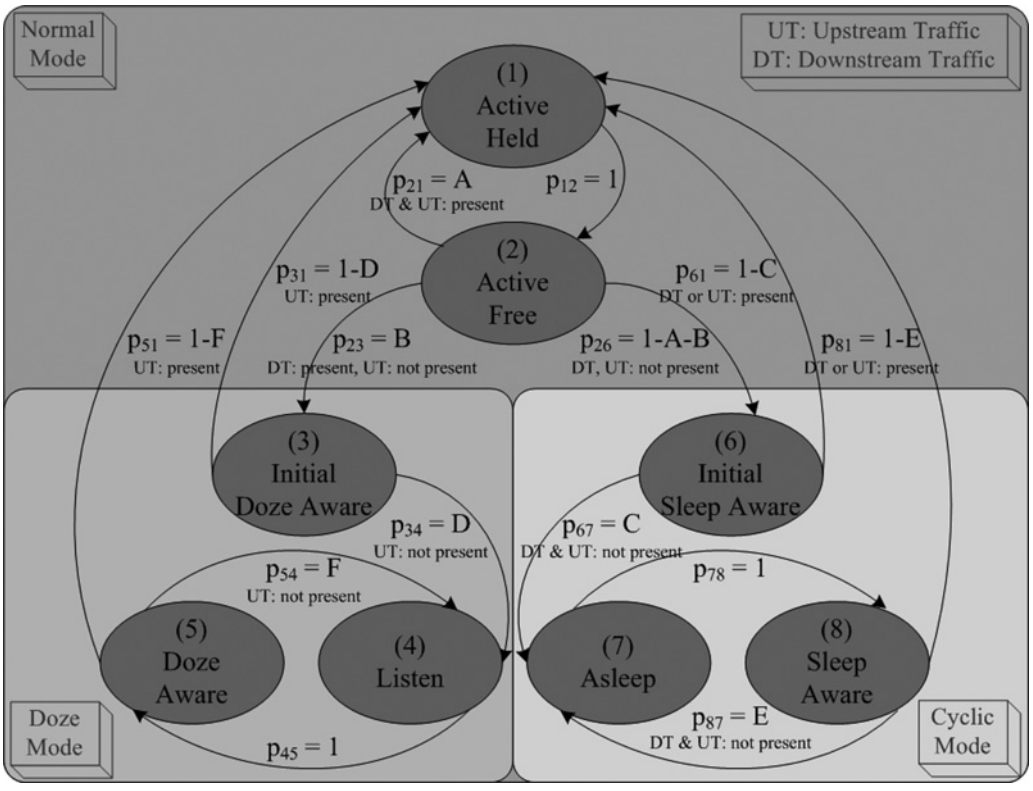

Fig. 3 *Proposed DTMC model*

Table 2 Traffic parameters

Scenario	Service	Direction	Metric	Value
first	Poisson arrival process	downstream	arrival rate (λ_d)	0.05:0.1:3 arrivals per 125 μs
			average burst size	1000 bytes
		upstream	arrival rate (λ_u)	0.05:0.1:3 arrivals per 125 μs
			average burst size	200 bytes
second	Poisson arrival process	downstream	arrival rate (λ_d)	0.05 arrivals per 125 μs
			average burst size	1000 bytes
		upstream	arrival rate (λ_u)	0.05:0.1:3 arrivals per 125 μs
			average burst size	200 bytes
third	Poisson arrival process	downstream	arrival rate (λ_d)	0.05:0.1:3 arrivals per 125 μs
			average burst size	1000 bytes
		upstream	arrival rate (λ_u)	0.05 arrivals per 125 μs
			average burst size	200 bytes
fourth	VoIP	downstream	average inter-arrival time ($1/\lambda_d$)	0.02 s
			average burst size	133 bytes
		upstream	average inter-arrival time ($1/\lambda_u$)	0.13 s
			average burst size	87 bytes
	real-time video	downstream	average inter-arrival time ($1/\lambda_d$)	0.003 s
			average burst size	1365 bytes
		upstream	average inter-arrival time ($1/\lambda_u$)	0.14 s
			average burst size	88 bytes
	streaming video	downstream	average inter-arrival time ($1/\lambda_d$)	0.001 s
			average burst size	1450 bytes
		upstream	average inter-arrival time ($1/\lambda_u$)	0.09 s
			average burst size	66 bytes

expresses the probability of the ONU being in a specific state of the DTMC after a long time or equivalently when the system reaches equilibrium. According to Chapman–Kolmogorov equations the following linear system holds

$$\boldsymbol{u} = \boldsymbol{u}\Xi \Rightarrow [u_1,\ u_2,\ \ldots,\ u_8] = [u_1,\ u_2,\ \ldots,\ u_8] \cdot \Xi \quad (3)$$

The algebraic multiplication of (3) yields the following eight equations

$$-u_1 + A \cdot u_2 + (1-D) \cdot u_3 + (1-F)u_5 + (1-C)u_6 + (1-E) \cdot u_8 = 0 \quad (4)$$

$$u_1 - u_2 = 0 \quad (5)$$

$$B \cdot u_2 - u_3 = 0 \quad (6)$$

$$D \cdot u_3 - u_4 + F \cdot u_5 = 0 \quad (7)$$

$$u_4 - u_5 = 0 \quad (8)$$

$$u_2 \cdot (1-A-B) - u_6 = 0 \quad (9)$$

$$C \cdot u_6 - u_7 + E \cdot u_8 = 0 \quad (10)$$

$$u_7 - u_8 = 0 \quad (11)$$

In addition, the following equation stands (the summation of all stationary probabilities is one)

$$u_1 + u_2 + u_3 + u_4 + u_5 + u_6 + u_7 + u_8 = 1 \quad (12)$$

By selecting nine equations, e.g. (4)–(12), the computation of the unknown variables becomes a straightforward task. In particular, assuming see (13)

the stationary probabilities are computed as follows
see (17) and (18) at the bottom of the next page

4.1 Average power consumption computation

Since the arrival-counting process is independently and exponentially distributed with the inter-arrival time gaps, a Poisson process is used to approximate the stationary probabilities [14, 16]. The upstream and the downstream arrival rates are expressed as λ_u and λ_d, respectively. $1/\lambda_u$ and $1/\lambda_d$ denote the inter-arrival time of data bursts at the UNI and the SNI, in accordance with the ITU-T recommendations [17]. Accordingly, for each time $t \in T$, the upstream ($\lambda = \lambda_u$) and the downstream ($\lambda = \lambda_d$) arrival probabilities are defined by $\Pr\{N(t) = i\} = (\lambda t)^i / i! e^{-\lambda t}$, $t \geq 0$, $i \in \mathbb{N}$. Therefore, the probabilities A, B, C, D, E, F can be expressed by the above Pr

$$\begin{aligned} &A - 2 \cdot C + 3 \cdot E + 2 \cdot A \cdot C + 2 \cdot B \cdot C - A \cdot E - 2 \cdot B \cdot D - A \cdot F \\ &\quad + 2 \cdot C \cdot F - 3 \cdot E \cdot F \cdot -2 \cdot A \cdot C \cdot F - 2 \cdot B \cdot C \cdot F + 2 \cdot B \cdot D \cdot E + A \cdot E \cdot F - 3 \neq 0 \end{aligned} \quad (13)$$

$$u_1 = u_2 = \frac{E + F - E \cdot F - 1}{\begin{aligned} &A - 2 \cdot C + 3 \cdot E + 2 \cdot A \cdot C + 2 \cdot B \cdot C - A \cdot E - 2 \cdot B \cdot D - A \cdot F \\ &\quad + 2 \cdot C \cdot F - 3 \cdot E \cdot F \cdot -2 \cdot A \cdot C \cdot F - 2 \cdot B \cdot C \cdot F + 2 \cdot B \cdot D \cdot E + A \cdot E \cdot F - 3 \end{aligned}} \quad (14)$$

$$u_3 = \frac{-B + B \cdot E + B \cdot F - B \cdot E \cdot F}{\begin{aligned} &A - 2 \cdot C + 3 \cdot E + 2 \cdot A \cdot C + 2 \cdot B \cdot C - A \cdot E - 2 \cdot B \cdot D - A \cdot F + 2 \cdot C \cdot F \\ &\quad - 3 \cdot E \cdot F \cdot -2 \cdot A \cdot C \cdot F - 2 \cdot B \cdot C \cdot F + 2 \cdot B \cdot D \cdot E + A \cdot E \cdot F - 3 \end{aligned}} \quad (15)$$

$$u_4 = u_5 = \frac{B \cdot D \cdot E - B \cdot D}{\begin{aligned} &A - 2 \cdot C + 3 \cdot E + 2 \cdot A \cdot C + 2 \cdot B \cdot C - A \cdot E - 2 \cdot B \cdot D - A \cdot F + 2 \cdot C \cdot F \\ &\quad - 3 \cdot E \cdot F \cdot -2 \cdot A \cdot C \cdot F - 2 \cdot B \cdot C \cdot F + 2 \cdot B \cdot D \cdot E + A \cdot E \cdot F - 3 \end{aligned}} \quad (16)$$

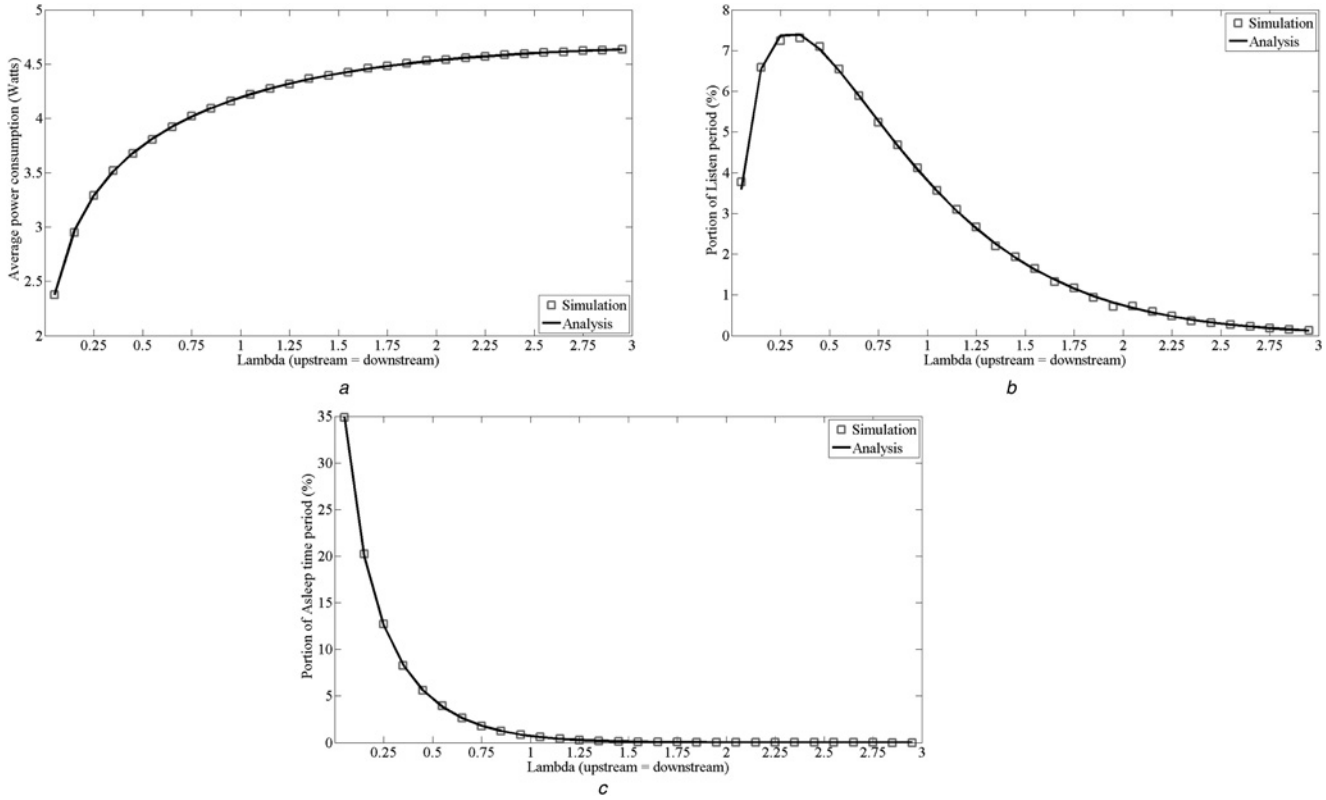

Fig. 4 *Scenario 1: performance evaluation when the upstream and downstream loads are increased identically*

a Scenario 1: average power consumption
b Scenario 1: portion of Listen period
c Scenario 1: portion of Asleep period

distributions as follows

$$A = 1 - e^{-\lambda_u \cdot T_{af}} \tag{19}$$

$$B = e^{-\lambda_u \cdot T_{af}} \cdot (1 - e^{-\lambda_d \cdot T_{af}}) \tag{20}$$

$$C = e^{-(\lambda_u + \lambda_d) \cdot T_{sa}} \tag{21}$$

$$D = e^{-\lambda_u \cdot T_{da}} \tag{22}$$

$$E = e^{-(\lambda_u + \lambda_d) \cdot (T_{sa} + T_{as})} \tag{23}$$

$$F = e^{-\lambda_u \cdot (T_{da} + T_{ls})} \tag{24}$$

Now, we are able to estimate the average power consumption of an ONU, denoted by P_c, in terms of watts, assuming that P_{ah}, P_{af}, P_{da}, P_{ls}, P_{sa}, P_{as} stand for the power consumed during the *ActiveHeld*, the *ActiveFree*, the *DozeAware*, the *Listen*, the *SleepAware*, and the *Asleep* states, and combining the stationary probabilities of (14)–(18)

$$P_c = u_1 \cdot P_{ah} + u_2 \cdot P_{af} + u_3 \cdot P_{da} + u_4 \cdot P_{ls} + u_5 \cdot P_{da} + u_6 \cdot P_{sa} + u_7 \cdot P_{as} + u_8 \cdot P_{sa} \text{ watts} \tag{25}$$

The total ONU power consumed in an XG-PON can be derived by individually summing the overall power consumed at all ONUs. In case the traffic handled by each ONU is identical, the total power consumed in an XG-PON is defined as

$$P_{total} = \sum_{i=1}^{M} P_c \text{ watts} \tag{26}$$

where M is the number of the ONUs in the XG-PON.

5 Model validation and discussion

5.1 Simulation environment and parameters

To validate the proposed model, we have implemented an event-driven simulator in MATLAB. The operation of an XG-PON system with 32 (identical) ONUs was simulated. Each ONU receives downstream traffic in the SNI and forwards upstream traffic from the UNI. Our paper was focused on the power behaviour of each ONU. Hence, the obtained numerical results were captured and then verified with the analytical ones based on our analytical formulas. The values of the parameters used to obtain numerical results are summarised in Table 1, where

$$u_6 = \frac{(E-1)\cdot(F-1)\cdot(A+B-1)}{\begin{array}{l} A - 2\cdot C + 3\cdot E + 2\cdot A\cdot C + 2\cdot B\cdot C - A\cdot E - 2\cdot B\cdot D - A\cdot F + 2\cdot C\cdot F \\ - 3\cdot E\cdot F\cdot -2\cdot A\cdot C\cdot F - 2\cdot B\cdot C\cdot F + 2\cdot B\cdot D\cdot E + A\cdot E\cdot F - 3 \end{array}} \tag{17}$$

$$u_7 = u_8 = \frac{-C + A\cdot C + B\cdot C + C\cdot F - A\cdot C\cdot F - B\cdot C\cdot F}{\begin{array}{l} A - 2\cdot C + 3\cdot E + 2\cdot A\cdot C + 2\cdot B\cdot C - A\cdot E - 2\cdot B\cdot D - A\cdot F + 2\cdot C\cdot F \\ - 3\cdot E\cdot F\cdot -2\cdot A\cdot C\cdot F - 2\cdot B\cdot C\cdot F + 2\cdot B\cdot D\cdot E + A\cdot E\cdot F - 3 \end{array}} \tag{18}$$

Table 3 Scenario 1: evaluation results and confidence intervals

Upstream lambda, λ_u	Average power consumption, W			Portion of Listen period, %			Portion of Asleep period (95%)		
	Analysis, W	Simulation, W	Confidence interval (95%)	Analysis, %	Simulation, %	Confidence interval (95%)	Analysis, %	Simulation, %	Confidence interval, %
0.05	2.37	2.38	±0.008	3.59	3.29	±0.52	34.98	34.65	±0.45
0.55	3.81	3.80	±0.009	6.49	6.63	±0.19	3.83	3.95	±0.14
1.05	4.22	4.22	±0.007	3.54	3.53	±0.09	0.59	0.57	±0.04
1.55	4.42	4.42	±0.005	1.62	1.62	±0.09	0.08	0.08	±0.018
2.05	4.54	4.54	±0.003	0.68	0.67	±0.03	0.01	0.01	±0.004
2.55	4.60	4.60	±0.002	0.27	0.26	±0.02	0	0	±0
2.95	4.63	4.63	±0.002	0.12	0.14	±0.02	0	0	±0

the state sojourn time as well as the power consumed in each state in terms of watts are specified [2, 3]. It is worth mentioning that all state time periods have been set equal to 125 μs, which is the duration of the physical downstream/upstream frame.

5.2 Validation scenarios and results

Four different scenarios have been defined based on different traffic profiles. The traffic parameters of the four scenarios are summarised in Table 2. In the first three scenarios, both upstream and downstream traffic arrivals are governed by a Poisson arrival process. The last scenario involves real traffic traces as an input to the simulator. In the first scenario, the power consumption of each ONU is examined when symmetrical traffic is used. The second scenario investigates the power profile of each ONU when the upstream arrival probability changes over time, whereas the downstream arrival probability is fixed. The third scenario keeps the upstream traffic stable, whereas the downstream traffic varies. In the first three scenarios, the average burst size (per ONU) is equal to 1000 and 200 bytes in the downstream and upstream directions, respectively. Thus, the maximum downstream (upstream) traffic rate reaches 45,000 (9000) bytes for all ONUs when λ_d (λ_u), meaning that all traffic requests are fulfilled within a downstream (upstream) frame. Thus, our initial assumptions (Section 4) are met. In the last scenario, real traffic traces have been used in order to assess the validity of the proposed model under real traffic conditions. In particular, traffic traces captured from (a) a voice over IP (VoIP) session, (b) a real-time video session, and (c) a streaming video session were utilised in the conducted simulations. The fourth scenario encloses three experiments. In the first experiment, each ONU uses a VoIP session. The VoIP session generates about 5.5 and 53 kbps in the upstream and the downstream directions, respectively. The second experiment studies the ONU behaviour when a real-time video is served. In this case, 5 kbps and 3.6 Mbps were generated in the upstream and the downstream directions, respectively. Finally, a streaming video session was used in the third experiment, where 5.8 kbps and 11.6 Mbps were produced in the upstream and the downstream directions, respectively.

Three different performance metrics are considered, i.e. the *average estimated power consumption of the ONU* in watts, the *average time the ONU spends in the Listen state*, and the *average*

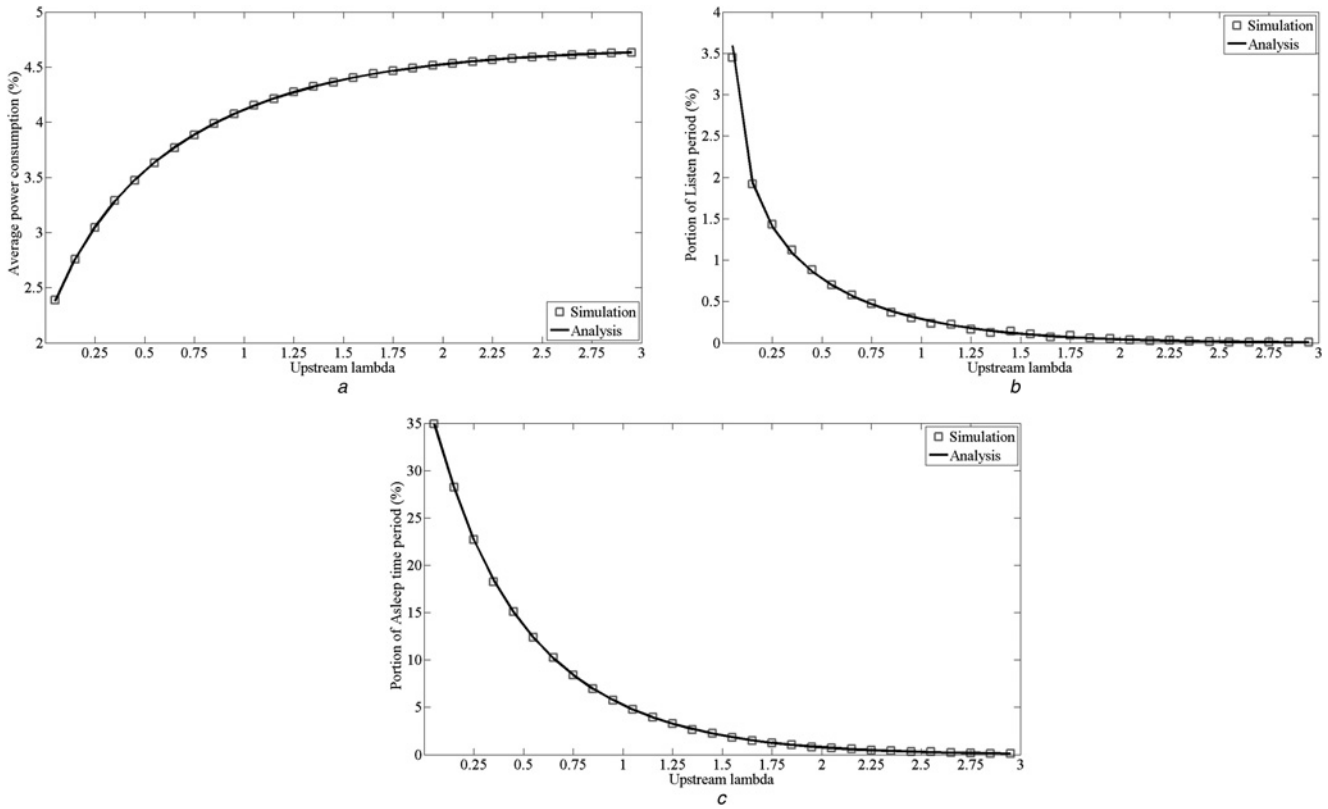

Fig. 5 *Scenario 2: performance evaluation when the downstream load remains stable and the upstream load is increased*

a Scenario 2: average power consumption
b Scenario 2: portion of Listen period
c Scenario 2: portion of Asleep period

Table 4 Scenario 2: evaluation results and confidence intervals

Upstream lambda, λ_u	Average power consumption, W			Portion of Listen period, %			Portion of Asleep period, %		
	Analysis	Simulation	Confidence interval (95%)	Analysis, %	Simulation, %	Confidence interval (95%)	Analysis, %	Simulation, %	Confidence interval (95%)
0.05	2.37	2.38	±0.008	3.59	3.82	±0.29	34.98	34.74	±0.34
0.55	3.63	3.64	±0.009	0.69	0.70	±0.05	12.35	12.25	±0.16
1.05	4.14	4.14	±0.007	0.26	0.28	±0.02	4.76	4.83	±0.11
1.55	4.40	4.39	±0.004	0.09	0.09	±0.02	1.84	1.90	±0.05
2.05	4.53	4.53	±0.002	0.04	0.04	±0.01	0.70	0.67	±0.03
2.55	4.60	4.60	±0.003	0.01	0.01	±0	0.26	0.26	±0.02
2.95	4.63	4.63	±0.002	0	0	±0	0.12	0.10	±0.02

time the ONU spends in the Asleep state. The results of the analytical framework are represented by the curve named as 'Analysis' and are compared with the simulation results, represented by the curve named as 'Simulation'. Regarding the *average estimated power consumption*, the analytical results have been produced based on (25). The *average time the ONU spends in the Listen and the Asleep states* is given by the stationary probability of the *Listen* and the *Asleep* states, respectively, multiplied by 100.

Concerning the first scenario, Fig. 4*a* depicts the average ONU power consumption in watts, Fig. 4*b* illustrates the average time the ONU spent in the Listen sleep mode, and Fig. 4*c* shows the average time the ONU experienced in the *Asleep* sleep mode. Table 3 depicts the exact numerical results and the corresponding 95% confidence interval intervals. As the probability of monitoring downstream and upstream traffic becomes higher, the number of transitions from high to low-power mode decreases. In particular, the transition probabilities p_{23} (to a potential doze mode) and p_{26} (to a potential cyclic sleep mode) are getting lower. As the arrival rates λ_d and λ_u increase, leading to increased probability of downstream and upstream traffic to be present, the transition probability p_{26} tends to zero, since

$$p_{26} = 1 - A - B = 1 - \left(1 - e^{-\lambda_u T_{af}}\right) - e^{-\lambda_u T_{af}} \cdot \left(1 - e^{-\lambda_d T_{af}}\right) = e^{-(\lambda_u + \lambda_d)\cdot T_{af}} \Rightarrow \lim_{\substack{\lambda_d \cdot \infty \\ \lambda_u \to \infty}} e^{-(\lambda_u + \lambda_d)\cdot T_{af}} = 0.$$

From Fig. 4*b*, it may be observed that the average time the ONU stays in the *Listen* state is maximised when $\lambda_u = \lambda_d \simeq 0.3$, reaching ~7.5%; thus, the stationary probability of being in *Listen* state is 0.075. As illustrated in Fig. 4*b*, the time period the ONU spends in doze mode is initially (until λ_d and λ_u reach 0.3) increased; this may be attributed to the fact that the probability of switching from *ActiveFree* state to the *Initial DozeAware* state (i.e. the transition probability p_{23}) gains ground, whereas the probability of transiting from the *ActiveFree* state to the *Initial SleepAware* state diminishes.

Fig. 5*a* shows the average ONU power consumption in the context of the second scenario, varying the upstream traffic. Table 4 summarises the exact numerical results and the corresponding 95% confidence interval intervals. The downstream arrival rate is

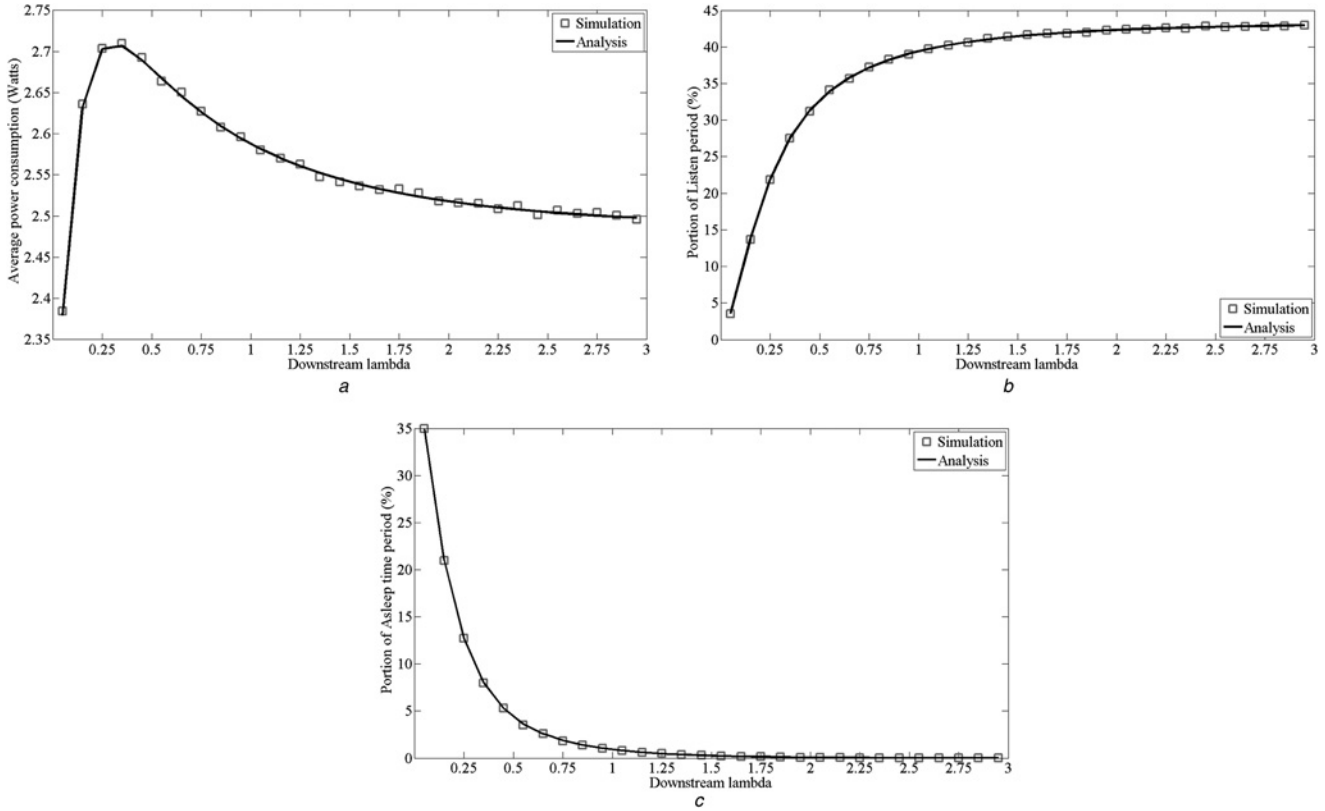

Fig. 6 *Scenario 3: performance evaluation when the upstream load remains stable and the downstream load is increased*

a Scenario 3: average power consumption
b Scenario 3: portion of Listen period
c Scenario 3: portion of Asleep period

IET Netw., 2016, Vol. 5, Iss. 3, pp. 71–79

Table 5 Scenario 3: evaluation results and confidence intervals

Downstream lambda, λ_d	Average power consumption, W			Portion of Listen period, %			Portion of Asleep period, %		
	Analysis, W	Simulation, W	Confidence interval (95%)	Analysis, %	Simulation, %	Confidence interval (95%)	Analysis, %	Simulation, %	Confidence interval (95%)
0.05	2.37	2.38	±0.005	3.59	3.52	±0.33	34.98	35.02	±0.32
0.55	2.66	2.67	±0.007	33.92	33.67	±0.40	3.63	3.70	±0.17
1.05	2.58	2.57	±0.006	39.71	39.87	±0.22	0.80	0.79	±0.05
1.55	2.53	2.54	±0.005	41.57	41.49	±0.16	0.23	0.25	±0.02
2.05	2.51	2.52	±0.003	42.37	42.23	±0.10	0.07	0.07	±0.01
2.55	2.50	2.50	±0.004	42.77	42.73	±0.12	0.02	0.02	±0
2.95	2.49	2.49	±0.003	42.95	43.00	±0.09	0.01	0	±0

Table 6 Performance results with real traffic traces

Service	Metric	Analysis	Simulation
VoIP	average *Power* consumption (watts)	1.99 W	2.02 W
	portion of *Listen* time period, %	19.22 %	20.35 %
	portion of *Asleep* time period, %	29.14 %	30.71 %
real-time video	average *Power* consumption, watts	1.84 W	1.84 W
	portion of *Listen* time period, %	0.01 %	0.02 %
	portion of *Asleep* time period, %	49.89 %	49.78 %
streaming video	average *Power* consumption, watts	1.84 W	1.85 W
	portion of *Listen* time period, %	0.04 %	0.03 %
	portion of *Asleep* time period, %	49.98 %	49.66 %

considered predefined and stable. Once more, the power required is increased as the traffic becomes more demanding, since fewer sleep opportunities appear. By observing Figs. 5*b* and *c*, which depict the average time the ONU spends in the *Listen* and the *Asleep* states, respectively, we can associate the ONU behaviour with the traffic present in both directions.

Concerning the third scenario, Figs. 6*a–c* show the ONU behaviour varying the downstream arrival rate. The third scenario considers a fixed very low upstream traffic for the whole experiment, whereas the first two scenarios assumed that the upstream traffic progressively increases. As a result, the ONU experiences a progressively reduced cyclic sleep mode as the downstream traffic gains ground. On the other hand, the fraction of time the ONU operates in doze mode is constantly increased, and as the downstream traffic reaches its upper bound, eventually overrules. This is attributed to the fact that the doze mode entails the absence of upstream traffic only; hence, a doze period establishment becomes increasingly possible as the downstream traffic grows being at the same time quite unlikely for the cyclic mode to occur. This phenomenon may be observed in Fig. 6*b*, where the average time the ONU spends in the *Listen* state continuously increases, reaching the value of 44%. At this time, the ONU experiences a sequential transition of *Listen–DozeAware* states, remaining almost exclusively in doze sleep mode (Table 5).

In the fourth scenario, the results of using real traffic traces are presented. Table 6 shows the results from the analysis and the simulation. For example, when all ONUs utilise a VoIP session the average power consumption is 1.99 and 2.02 W based on the analytical and the simulation results, respectively. Accordingly, the portion of the Listen time period is 19.22% based on the analytical results and 20.35% based on the simulation results. Moreover, the portion of the Asleep time period is 29.14% in the analysis and 30.71% in the simulation. When using a VoIP session, the error rate of the proposed model is quite low, that is, about 5%. When a real-time video session is utilised in the XG-PON, the acquired results is similar. Analysis and simulation results are totally agreed when the average power is measured.

6 Conclusion

In this paper, a precise model was presented analysing the ONU power management in XG-PON systems. The model consists of a DTMC, which encloses a set of countable states that describe the power management states of an ONU. The proposed analytical framework focused on the ONU average power consumption estimation, assuming that the ONU is able to support both the doze and cyclic sleep modes. Extensive validation and evaluation results are presented, reflecting the model's accuracy. Concurrently, the average power consumption, the average time spent in the *Listen* state, and the average time spent in the *Asleep* state were associated to the traffic an ONU experiences in both directions.

7 Acknowledgment

This work was supported by the Internship of Excellence granted by the Department of Informatics, Aristotle University of Thessaloniki in the project title: 'Reduction of Energy Consumption in Passive Optical Networks'.

8 References

1 Effenberger, F.J., El-Bawab, T.: 'Passive optical networks (PONs): past, present, and future', *Opt. Switch. Netw.*, 2009, **6**, (3), pp. 143–150
2 ITU-T G.987.3: '10-Gigabit-capable passive optical networks (XG-PON): transmission convergence (TC) specifications', 2010
3 ITU-T G.Supplement 45: 'GPON power conservation', 2009
4 Yi, Z., Chowdhury, P., Tornatore, M., *et al.*: 'Energy efficiency in telecom optical networks', *IEEE Commun. Surv. Tutor. Fourth Quarter*, 2010, **12**, (4), pp. 441–458
5 Zhang, J., Ansari, N.: 'Toward energy-efficient 1G-EPON and 10G-EPON with sleep-aware MAC control and scheduling', *IEEE Commun. Mag.*, 2011, **49**, (2), pp. s33–s38
6 Kubo, R., Kani, J.I., Fujimoto, Y., *et al.*: 'Adaptive power saving mechanism for 10 gigabit class PON systems', *IEICE Trans. Commun. Mag.*, 2010, **E93-B**, (2), pp. 280–288
7 Kubo, R., Kani, J.I., Ujikawa, H., *et al.*: 'Study and demonstration of sleep and adaptive link rate control mechanisms for energy efficient 10G-EPON', *IEEE/OSA J. Opt. Commun. Netw.*, 2010, **2**, (9), pp. 716–729
8 Shi, L., Mukherjee, B., Lee, S.S.: 'Energy-efficient PON with sleep-mode ONU: progress, challenges, and solutions', *IEEE Netw.*, 2012, **26**, (2), pp. 36–41
9 Valcarenghi, L.: 'Cognitive PONs: a novel approach toward energy efficiency'. Proc. Asia Communications and Photonics Conf. (ACP), Hong Cong, China, November 2012, pp. 1–3
10 Valcarenghi, L., Cerutti, I., Castoldi, P.: 'Energy efficient multicasting in TDMA PONs', *J. High Speed Netw.*, 2012, **18**, (4), pp. 213–222
11 Dhaini, A.R., Pin-Han, H., Gangxiang, S.: 'Toward green next-generation passive optical networks', *IEEE Commun. Mag.*, 2011, **49**, (11), pp. 94–101
12 Shing-Wa, W., Valcarenghi, L., She-Hwa, Y., *et al.*: 'Sleep mode for energy saving PONs: advantages and drawbacks'. Proc. IEEE GLOBECOM Workshops, Honolulu, HI, USA, November–December 2009, pp. 1–6
13 Sarigiannidis, P.G., Pechlivanidou, V.D., Louta, M.D., *et al.*: 'Towards an effective energy efficient passive optical network'. Proc. IEEE Symp. on Computers and Communications (ISCC), Corfu, Greece, June 2011, pp. 391–396
14 Chen, S., Dhaini, A.R., Ho, P.H., *et al.*: 'Downstream-based scheduling for energy conservation in green EPONs', *J. Commun.*, 2012, **7**, (5), pp. 400–408
15 Bang, H., Kim, J., Lee, S.S., *et al.*: 'Determination of sleep period for cyclic sleep mode in XG-PON power management', *IEEE Commun. Lett.*, 2012, **16**, (1), pp. 98–100
16 Bang, H., Kim, J., Shin, Y., *et al.*: 'Analysis of ONT buffer and power management performances for XG-PON cyclic sleep mode'. Proc. IEEE Globecom, Anaheim, CA, USA, December, 2012, pp. 3116–3121
17 ITU-T G.988: 'ONU management and control interface (OMCI) specification', 2010